Modeling the Dynamic Responses of Riparian Vegetation and Salmon Habitat in the Oregon Coast Range With State and Transition Models

Steven M. Wondzell, Agnieszka Przeszlowska, Dirk Pflugmacher, Miles A. Hemstrom, and Peter A. Bisson

Authors

Steven M. Wondzell is a research aquatic ecologist, Forestry Sciences Laboratory, 3625 93rd Avenue SW, Olympia, WA 98512-9193, swondzell@fs.fed.us. **Agnieszka Przeszlowska** is a research ecologist, Forestry Sciences Laboratory, 3625 93rd Avenue SW, Olympia, WA 98512-9193, agnesp@gmail.com. **Dirk Pflugmacher**[1] graduate research assistant, Department of Forest Ecosystems and Society, Oregon State University, 321 Richardson Hall, Corvallis, OR 97331, dirk.pflugmacher@geo.hu-berlin.de. **Miles A. Hemstrom**[2] is a research ecologist (retired), Forestry Sciences Laboratory, 620 SW Main St. Portland, OR 97205. **Peter A. Bisson** is a research fish biologist, Forestry Sciences Laboratory, 3625 93rd Avenue SW, Olympia, WA 98512-9193, pbisson@fs.fed.us.

Abstract

Interactions between landuse and ecosystem change are complex, especially in riparian zones. To date, few models are available to project the influence of alternative land-use practices, natural disturbance and plant succession on the likely future conditions of riparian zones and aquatic habitats across large spatial extents. A state and transition approach was used to model the effects of various management and restoration practices on conditions of riparian forests, channel morphology, and salmonid habitat. We present results of model analyses for the Wilson River in the Oregon Coast Range. We focus on critical habitat for spawning and rearing salmon and how habitat quality might be influenced by alternative land-use practices over the next 50 years, especially contrasting the outcomes of passive vs. active habitat restoration strategies. Results of our simulations suggest that active restoration of large wood in streams may accelerate habitat improvement relative to recovery projections under a passive restoration strategy. Active restoration seems to be a more viable approach for species such as coho salmon in the Wilson River watershed, which has limited potential spatial distribution in the drainage network, and where a significant proportion of the available habitat is in poor condition. In contrast, using active restoration techniques to improve habitat for a widely distributed species such as steelhead seems less feasible. Steelhead habitat is abundant throughout the basin and at least some of it is currently in good or excellent condition. Thus, large portions of the Wilson River would need to be restored to substantially increase the proportion of the stream network that is in good or excellent condition for steelhead.

Very little data are available with which to validate models at this scale. Results of our model simulations appeared reasonable wherever field and lidar data were available for comparison, however we caution that these comparisons do not validate all the factors simulated in our models. Consequently, the results of the model simulations should be interpreted as hypotheses of likely outcomes from management strategies at the scale of a large watershed (one or several 5th-field hydrologic units or HUC5s) or a large portion of a USFS ranger district. Nevertheless, the approach holds promise for simulating physical and biological responses of aquatic organisms and their habitats to alternative restoration approaches.

Keywords: state and transition models, riparian management, stream habitat, Oregon Coast Range, Tillamook burn, large wood addition, coho, steelhead, lidar.

[1] Now at Department of Geography, Humboldt University of Berlin, Unter den Linden 6, 10099 Berlin, Germany.
[2] Now at Institute for National Resources, Oregon State University, Portland, Oregon, miles.hemstrom@oregonstate.edu.

Introduction

Pacific salmon and steelhead have declined in abundance or have been eliminated from large parts of their historical range (Nehlsen et al. 1991), and many populations are now listed under the U.S. Endangered Species Act (USDA and USDI 2000). Multiple factors have contributed to these declines, including the degradation of spawning and rearing habitat in tributary streams (Federal Caucus 2000). Maintenance of existing high-quality habitat and restoration of degraded habitat have become cornerstones of many salmon recovery efforts (NRC 2002). However, there is a critical need for information relating how management activities in riparian areas will interact with natural processes to create and maintain salmon habitat and how this habitat will change over time—particularly over the broad spatial extents that are relevant to recovering salmonid populations. Landscape-scale perspectives of historical, current, and potential future conditions of upland, riparian, and aquatic systems resulting from plant succession, natural disturbances, and land-use practices can help inform policy directions. Further, such information is essential to developing strategic restoration policies for large regions (e.g., Oregon Plan for Salmon and Watersheds; http://www.oregon-plan.org/ accessed 15 November 2011) that make the most of limited funds. However, providing relatively detailed information on current and future riparian conditions for large watersheds (e.g., one or several 5th-level hydrologic units sometimes referred to as HUC5 or HUC6 watersheds; USGS and USDA, 2009) over large areas poses substantial logistical and technical challenges.

Mapping and classifying riparian zones using a combination of remotely sensed and field-collected data offers a means of assessing the current condition of riparian areas at fine detail over large areas. However, these assessments only provide a static "snapshot" of a watershed at a single point in time. The objective of this project was to develop state and transition models that could use this "snapshot" as a starting point and then project changes in salmonid habitat resulting from ecological processes that shape streams, riparian vegetation, and the upland systems to which they are connected.

The state and transition models developed here were designed to forecast changes at the watershed scale (one to several 5th-field HUCs) resulting from plant succession, hydrogeomorphic processes, and natural disturbances. Simulations using a background natural disturbance regime were used to "hindcast" the historical condition and to forecast the outcomes of "passive restoration", i.e., the strategy of allowing natural ecosystem processes to dictate the pace and trajectory of habitat recovery without human intervention. The models also accommodate land use activities such as logging, stream and riparian restoration activities (e.g., large wood additions to streams or planting of conifers in riparian areas to facilitate conversion from hardwoods to conifer dominated stands), and episodic disturbance events (e.g., debris flows, windthrow, and wildfires) that shape stream channels and valley floors. The models were used to forecast the outcome of alternative management policies, specifically contrasting a passive restoration strategy to an active strategy of restoring large wood to forested stream reaches where large, in-stream wood is currently lacking.

Methods

The aquatic-riparian state and transition models described in this paper were designed to simulate the temporal dynamics of riparian vegetation in the mountain stream networks of the Oregon Coast Range. To apply these models, the stream network must be delineated into relatively homogeneous stream reaches classified into "potential geomorphic types." The riparian zone around each reach must then be mapped and assigned to a "potential vegetation type." Each reach polygon must also be attributed with the current vegetation type to provide a starting point for the model simulation. These steps are described, below. Additional information on the methods we used, along with the aquatic-riparian state and transition models and supporting data are available from the project website (accessed 7 November, 2011): http://www.fs.fed.us/pnw/lwm/aem/projects/ar_models.html.

Stream Network Delineation and Classification

The stream network was delineated with the NetStream

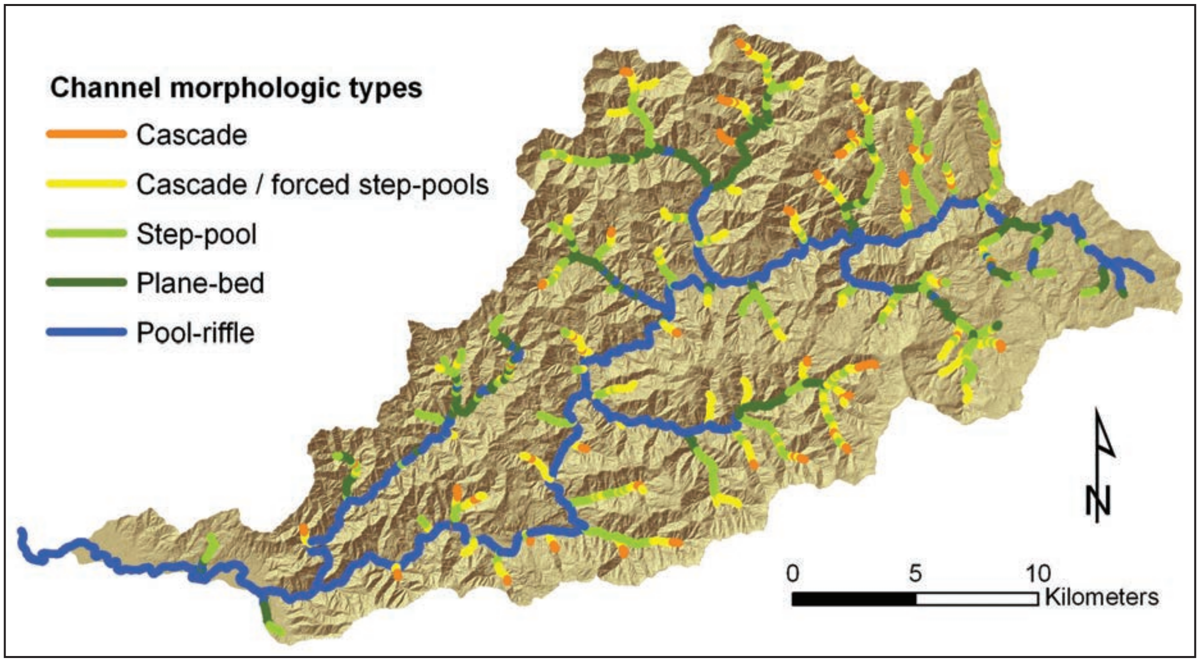

Figure 1—Classification of stream reaches into potential geomorphic types following the stream classification system of Montgomery and Buffington (1997 and 1998).

tool available from Earth Systems Institute[3] and hydraulic geometry coefficients for Pacific maritime mountain streams (Castro and Jackson 2001). A 5-m Lidar DEM and literature derived threshold values for drainage area and channel gradient were used to trace the stream network and provide a preliminary classification of channel reaches into six geomorphic types described by Montgomery and Buffington (1997, 1998): (1) colluvial, (2) cascade, (3) cascade with wood-forced step-pools, (4) step-pool, (5) plane-bed, and (6) pool-riffle (fig. 1). We dropped non-fish-bearing stream reaches from our analysis (i.e., bedrock and colluvial reaches and those with channel gradient > 20 percent or drainage areas < 1.5 km^2). We compared our preliminary classification with field-classified geomorphic types from 29 sampled reaches (described below). The final classification correctly assigned 86 percent of the 29 sampled reaches in the Wilson River watershed into their respective Montgomery and Buffington potential geomorphic types. The final stream network was generated with field-derived coefficients for bankfull width and depth and the boundary of the riparian zone around each classified stream reach was then delineated using path-distance thresholds generated from ArcGIS path-distance tools. This method identifies a geomorphically delineated riparian zone based on a "cost threshold" evaluated from a combination of distance and elevation from the active channel. We verified riparian zone delineations by comparing the path-distance derived boundaries to boundaries mapped at our 29 field sites based on distance, elevation, and slope breaks to adjacent hillslopes.

The geomorphically defined riparian zone boundary is likely to underestimate the influence of stream-adjacent trees in areas where steep hillslopes bound narrow valley floors. In these locations, trees growing on lower hillslopes may significantly affect riparian conditions in the stream. Thus, the limits of the riparian polygons were defined in two ways: the actual valley-floor delineation was done using the path-distance methods described above and a 30-m

[3] These tools are available from the NETMAP website: http://www.netmaptools.org.

Note: The use of trade or firm names in this publication is for reader information and does not imply endorsement by the U.S. Department of Agriculture of any product or service.

Table 1—Cross-walk between upland potential vegetation types (PVTs), plant association groups (PAGs), and the final riparian PVTs used for our model development within the Wilson River watershed

Riparian PVT	PAG description	PAG code	Upland PVT description
not modeled	Sitka spruce/ wet nonforest	991	nonforest
not modeled	W. hemlock/dry non-forest	1971	nonforest
not modeled	W. hemlock/wet non-forest	1991	nonforest
Sitka spruce/W. hemlock wet	Sitka spruce/oxalis-swordfern-moist	902	Sitka spruce (coastal)
Sitka spruce/W. hemlock wet	Sitka spruce/salal-mesic	901	Sitka spruce (coastal)
Sitka spruce/W. hemlock wet	Sitka spruce/salmonberry-wet	903	Sitka spruce (coastal)
Sitka spruce/W. hemlock wet	W. hemlock/oxalis-swordfern-moist	1907	W. hemlock moist (cascades)
Sitka spruce/W. hemlock wet	W. hemlock/salmonberry-wet	1908	W. hemlock wet (coastal)
W. hemlock intermediate	Pacific silver fir/Alaska huckleberry-wet	2207	silver fir intermediate (high)
W. hemlock intermediate	Pacific silver fir/oxalis-high precipitation	2208	silver fir intermediate (high)
W. hemlock intermediate	W. hemlock/Alaska huckleberry/oxalis	1909	W. hemlock cool (cascades)
W. hemlock intermediate	W. hemlock/Oregon grape-salal	1906	W. hemlock intermediate (cascades)
W. hemlock intermediate	W. hemlock/vanilla leaf-cool	1905	W. hemlock cool (cascades)
W. hemlock intermediate	W. hemlock-warm, transitional to Douglas fir	1903	W. hemlock hyperdry (SW)

buffer was also drawn on both sides of the stream. The final "riparian" polygon used for vegetation classification was defined as the larger of the two methods.

Potential Riparian Vegetation

We based our classification of riparian potential vegetation types (PVT) on the adjacent plant association groups (PAGs obtained from the Northwest Oregon Ecology Group, Corvallis, Oregon) and upland PVTs from the Siuslaw National Forest, Oregon (table 1) because potential vegetation type spatial data with previously classified riparian vegetation were not available. The dominant PVTs in the Wilson River watershed are Sitka spruce/western hemlock wet PVT and Douglas fir/western hemlock PVT. We added a meadow riparian PVT to characterize riparian areas in the northeast portion of the Wilson watershed where deep-seated landslides created low gradient valleys with high water tables, and present-day flooding by beaver dams tends to prevent forested vegetation types. The meadow riparian PVT is characterized by PAGs in the Douglas-fir/western hemlock PVT as well as alder, willow and sedge functional groups. Combining the 3 PVTs with the potential geomorphic types (figure 1) resulted in a suite of 11 separate state and transition models for the Wilson River watershed (table 2).

Field Sampling of Selected Reaches

Sampling was designed to characterize three aspects of selected study reaches: (1) channel, steambank, and valley floor geomorphic conditions of the entire reach; (2) vegetation zones within the reach; (3) vegetation composition and structure in quantitative sub-plots. We randomly selected a stratified sample of 30 stream reaches from the preliminary delineation and classification. We generated fine-scale hillshade and canopy height maps for each reach and field sampling protocols were designed around these maps. We sampled 29 of these reaches during the summer of 2009 to provide data from which current conditions could be classified and mapped for the entire stream network within the study watershed.

Channel and valley floor geomorphic conditions— At each reach, the channel morphology was classified into channel types following the Montgomery and Buffington (1997, 1998) classification. Similarly, the overall plant association group and potential vegetation type was determined and the current vegetation structure was classified following state-classes as defined in the state and transition models (described below). Current land use, evidence of herbivory, and the overall condition of the channel were also noted. The longitudinal gradient was measured using an auto-level

Table 2—List of the 11 aquatic-riparian state and transition models developed for the Wilson River watershed.

Model	Potential vegetation type	Channel type	Length (km)	Riparian area (ha)	Percent total length	Percent total riparian area
sx_cscd	Sitka spruce	Cascade	4.1	27.4	2	2
sx_cscd_sp	Sitka spruce	Cascade / w-f step-pools	28.1	174.1	12	13
sx_sp	Sitka spruce	Step-pool	43.0	262.1	19	19
sx_pb	Sitka spruce	Plane-bed	26.8	162.6	12	12
sx_pr	Sitka spruce	Pool-riffle	35.1	212.9	16	15
me_pr	Meadow	Pool-riffle	11.7	70.4	5	5
df_cscd	Western hemlock	Cascade	6.2	40.2	3	3
df_cscd_sp	Western hemlock	Cascade / w-f step-pools	18.7	114.2	8	8
df_sp	Western hemlock	Step-pool	31.4	192.4	14	14
df_pb	Western hemlock	Plane-bed	12.4	75.2	6	5
df_pr	Western hemlock	Pool-riffle	7.4	44.4	3	3
		Grand total	224.9	1,375.9	100.0	99.0

Note: "w-f" in "Cascade / w-f step pools" denotes "wood-forced" – steep channels where steps and pools are formed where large wood obstructs the channel and that, lacking wood, would otherwise have a cascade morphology.

and stadia rod. Measurements were taken over a 100-m long length of channel wherever possible although dense vegetation sometimes limited the survey length.

The limits of both the active valley floor and the total valley floor were delineated on the hillshade and canopy height maps. We defined the active valley floor as the area with flood return intervals of 2 to 5 years, and determined the limits of this zone based on evidence of scouring, sediment deposition, and vegetative change outside of the bankfull width of the channel. We defined the total valley width as the limit of valley floor inundation which might occur in a 100-year return interval flood. Practically, the total valley floor width was determined by distance from, and height above, the bankfull channel and often coincided with obvious slope breaks with adjacent hillslopes or terraces.

Within each reach, we established five cross-channel transects which were marked on the hillshade and canopy height maps. The first transect was located randomly, using a random number generator, and located within the first 20 percent of the reach length. The remaining transects were spaced at equal intervals along the remaining 80 percent of the reach length. All pools, pool-structure, large wood, and over-hanging vegetation was inventoried between transects 1 and 5. The length, type, forming agent, total depth, tail-out depth (residual depth by difference) was recorded for each pool. All pieces of large wood were also inventoried. Lengths and diameters of each piece of large wood, in or suspended above, the bankfull channel, were estimated and a subset was measured. Also, we recorded percent of total length of large wood within the bankfull channel and the proportion that would be in the water at bankfull flows.

We measured the bankfull width, right and left bank elevation, thalweg depth, and two additional bed depths to provide a coarse cross-sectional profile at each cross-channel transect. Bankfull depth was calculated as the difference between the bankfull elevation and the thalweg depth. The elevation measurements were made using a stadia rod and inclinometer and provided reasonably accurate measurements (a system we field tested at the beginning of the field season and provided repeatable elevation measurements accurate to within a few centimeters). Bank characteristics were recorded for both the left and right banks, for a 2-m wide swath centered on the transect tape (1-m upstream and 1-m downstream). Within this zone, the stream bank was ranked either as stable or unstable. The percent length of undercut bank and average undercut depth was also recorded as was the ground cover on the bank and the percent of the swath with overhanging vegetation. Stream shade was evaluated at the center of the channel by estimating the percent of sky obscured by vegetation within a 20-cm diameter ring, held at arm length, 60° above a level horizon facing due south (the approximate location of the sun at solar noon on the solstice at the latitude of the study sites).

Reach and sub-reach summaries of vegetative conditions—
While in the field, discrete, homogenous vegetation zones within each study reach were delineated and mapped based on composition, size and structure of vegetation. We distinguished the following vegetation strata within each zone: (1) upper or overstory canopy layer; (2) secondary canopy layer; (3) sapling and tall-shrub layer (2 to 6-m height); (4) short shrub layer (0.5 to 2-m height); (5) herbaceous layer (<0.5 m); and (6) exposed ground. The total canopy cover and the relative cover by species were recorded for each layer. For tree layers the mean diameter breast height (DBH) was recorded from a subsample of trees present; for the shrub layers, average shrub heights were recorded. Herbaceous cover was characterized by functional groups (grasses, sedges, rushes, forbs, and ferns) rather than species. Ground cover was the percent of area not covered by herbaceous vegetation (soil, litter, rock/boulder, wood, water). Herbaceous and ground cover sum to 100 percent.

Quantitative sub-plots of vegetation composition and structure—
Eight to ten quantitative sub-plots were located in each study reach and data from these were used to develop lidar classification techniques for vegetation mapping. To allocate field plots, lidar canopy height rasters were segmented using eCognition software and classified into height classes. Field plot locations were then randomly selected based on height classes. These locations were then mapped onto the hillshade and canopy height maps for use in the field. Plots were located in the field using handheld GPS units and the detailed maps and then sampled to characterize the structure and composition of the vegetation within each sub-plot. The actual number of plots sampled was limited by the time available to sample each reach, but at least 5 of the 10 sub-plots were always sampled. We used sub-plots of 3 sizes: 5-m radius for tree plots; 2-m radius for shrub plots; 1-m radius for herbaceous plots. On tree plots, we recorded the species and DBH of all trees with DBH greater than 12.5 cm. We measured tree heights of at least 3 trees within each of three canopy layers (when present): (1) the upper or overstory canopy layer; (2) the secondary canopy layer; (3) the sapling layer. For trees between 2.54 and 12.5 cm DBH, all stems were counted and the mean height of the trees was estimated. For shrub plots, the mean height, canopy cover and species composition was recorded. For herbaceous plots, the height, cover, and composition were recorded. Dominant species were identified to species if possible.

Mapping Current Vegetation

To derive detailed information on current vegetation composition and structure for each riparian polygon we followed a two-step approach. First, using discrete-return lidar data (>8 pulses m^{-2}), a high-resolution raster map was created with a spatial resolution of 5 m. The map classification consists of 12 classes: 5 non-tree classes (water, barren, herbaceous vegetation, shrubs) and 7 tree classes distinguishing between conifer and hardwood, and tree sizes. For the tree classes an additional sub-class was derived separating stands with and without understory. In the second step, we calculated the area proportions of each (raster) class within each riparian polygon, and then labeled each polygon using a defined classification logic. Here, we briefly describe the classification methods and results. A more detailed description lies outside the scope of this paper which is focused on using state-and-transition models to simulate the dynamics of riparian vegetation.

The vegetation raster map was classified using measurements from the quantitative vegetation sub-plots for model training and validation. For each field plot, we extracted lidar point clouds and calculated 41 potential predictor variables from the lidar height and intensity distributions similar to Hudak et al. (2008). For estimation of continuous variables such as tree DBH we used multiple linear regression and for classification of categorical map attributes we used RandomForest (Breimann 2001). First, we used a canopy height model (fig. 2) and a height threshold of 0.5 m to separate woody vegetation (shrubs and trees) from herbaceous vegetation, barren, and water. Then we classified herbaceous vegetation, barren surfaces, and water

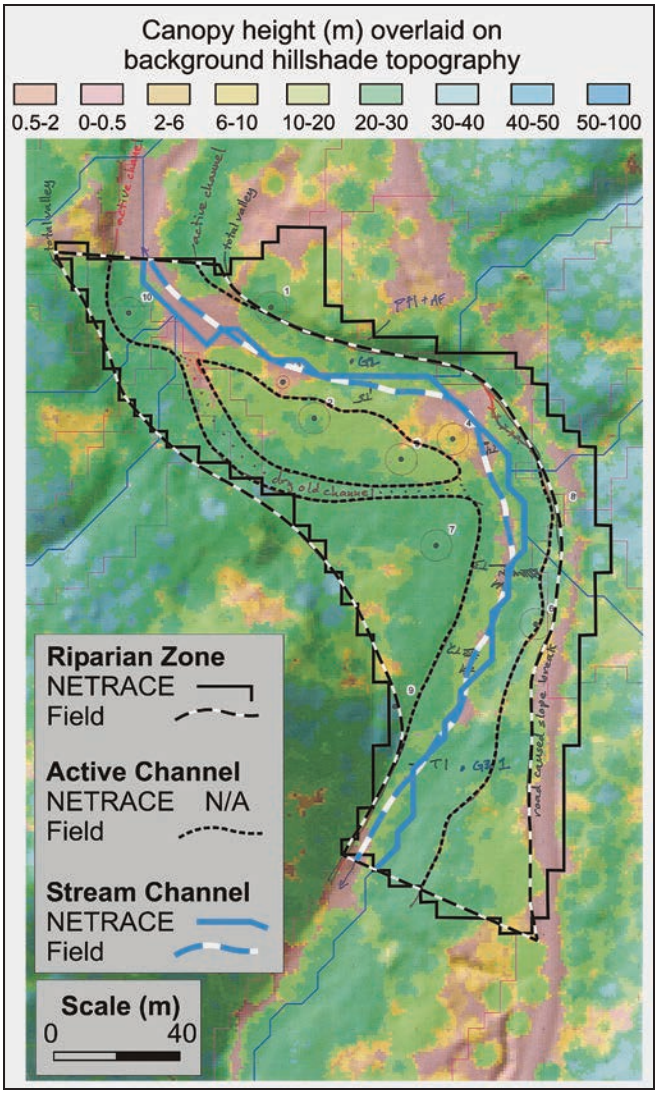

Figure 2—Example of a lidar-derived canopy height map overlaid on a hillslope-shaded topographic map prepared for field sampling a selected reach on the South Fork Wilson River. Lines contrast preliminary NetStream delineations (solid) with field-drawn delineations (white-dashed). Note, the right boundary of the riparian zone is caused by a road grade.

using lidar height and intensity metrics. However, low-stature shrubs (< 0.5 m) could not be reliably distinguished from herbaceous vegetation.

We then used the lidar-point data to estimate tree height and compared those estimates to the field-measured tree heights which showed a strong correlation for both conifers (r = 0.91) and hardwoods (r = 0.85). Because structural states in the state-and-transition models are based on tree diameters rather than height, tree height and canopy cover data derived directly from lidar were converted to tree diameter at breast height, using the following equations for hard woods and conifers:

$$dbh_H = \exp(0.537+0.147 * \mathrm{H95PCT}_{log} + 0.809 * \mathrm{HMEDIAN}_{log} + 0.003 * CANCOV)$$

$$dbh_c = \exp(0.2127 + 1.1045 * \mathrm{H95PCT}_{log})$$

Where dbhH and dbhC is maximum plot-level dbh for hardwoods and conifers, respectively, H95PCT is the 95th percentile of lidar vegetation heights, HMEDIAN, median lidar height and CANCOV is lidar canopy cover (number of returns above 2m divided by total number of returns). Model accuracy was acceptable (RMSE = 30-36 percent), but generally lower than observed in studies of more uniform forest stands. When converted to categorical size classes, overall classification accuracy was 64 percent (63 percent for hardwoods and 64 percent for conifers). For conifer trees, confusion (omission/commission error) between medium and large tree classes was roughly 40 percent, but balanced. For hardwood plots, there was a tendency of large trees to be mapped as medium tree class. Further, tall shrubs were misclassified as young hardwood trees. Thus, we combined the two classes into a single class.

A classification of hardwood and conifer forests was derived from lidar metrics using a combination of field and photo-interpretation plots. Analysis of the field data alone showed high omission errors for conifers, partly resulting from an unbalanced data set dominated by hardwood plots. Thus, to increase sample size, we collected additional reference data by means of photo-interpretation of near-infrared airphotos from the National Agriculture Imagery Program (NAIP). We generated 150 random plots (5 m diameter), 75 within and 75 outside the riparian zone. The best RandomForest model showed an overall accuracy of 85 percent (out-of-bag, boot-strapping estimate). Classification of tall understory shrubs showed an overall accuracy of 67 percent.

To estimate canopy density, we used lidar-derived estimates of canopy cover (vegetation returns above 2 m divided by all returns) without any transformation. We were unable to derive an acceptable relationship between tree cover estimates from the quantitative sub-plots and the lidar-derived canopy cover. However, at the polygon level the agreement between simple (uncalibrated) lidar cover and field-based estimates was high (80 percent).

To derive the current vegetation layer for the state-and-transition modeling, the vegetation raster map was summarized to describe the vegetation within each riparian polygon. Polygons were classified into bare (<=15 percent herbaceous) or herbaceous (>15 percent) when the proportion of shrub pixels within the valley floor polygon was less than 5 percent, or open (5–15 percent), medium (15–40 percent), and dense shrub (40–100 percent) otherwise. To account for a wider influence zone for trees we summarized forest structure attributes using a buffer zone of 30 m for stream orders 1–4, and a 30-m buffer in addition to the valley floor boundary for stream orders greater than 5. Here, we distinguished between nonforest (<15 percent), open forest (>15 percent) and dense forest (>40 percent). Forest polygons were classified as mixed conifer/hardwood when neither of the two forest types made up greater than 65 percent of the forest area. Further, we defined multi-layer stands when more than one tree size class occupied greater than 10 percent of the area. Canopy density was derived from lidar estimates of canopy cover (the number lidar returns above 2 m divided by the total number of returns) without any transformation.

The classification description for each riparian polygon was compared to the classification made during the field visit (table 3). The attributes of the overstory tree canopy were classified correctly approximately two-thirds of the time. However, the lidar-based methods had difficulty classifying understory attributes. The density of the understory shrub canopy agreed with the field observations in only 38 percent of the cases. Similarly, the agreement in the number of canopy layers was only 48 percent at the polygon level. In eight of the 10 erroneous classifications, the lidar failed to detect a multistory canopy observed in the field.

It is quite difficult to assess the overall classification accuracy. The lidar-based classification of the overstory tree types were quite accurate for homogeneous forest types (either conifer or hardwood) as evidenced by the 85 percent accuracy for the quantitative sub-plots. Summarizing the 5-m raster map to describe the heterogeneous riparian polygons was more challenging. For example, in only 3 of the 29 sampled plots (10 percent) did the lidar classification of all 5 attributes completely agree with the field classification. In only 8 of 29 plots (41 percent) did all 4 canopy attributes (excluding shrub canopy density) agree between the lidar and field classifications (table 3).

While the overall classification accuracy appears quite low, it does not distinguish between classification errors among ecologically similar classes (e.g., medium hardwood and large hardwood) and distinctly different classes (herbaceous versus forest). Overall, misclassified polygons tended to be classified into relatively similar classes (table 3). For example, in the hardwood plots, the regression equations relating height and diameter resulted in a tendency to map large diameter alders as medium diameter. While the lidar data were quite accurate in assessing canopy height, converting height to diameter classes added additional uncertainty caused by large variations in tree physiognomy. Similarly, the field sampling included 4 polygons with mixed conifer-hardwood overstory, of which, 3 were correctly classified by lidar. But the lidar also classified 6 hardwood or shrub dominated polygons as mixed. Thus, misclassified polygons were often classified into relatively similar classes.

The assessment of overall classification accuracy is further complicated because we do not have an accuracy assessment of our field classifications. Some attributes were easily observed in the field, but others were quite difficult to estimate. Estimating average canopy density for multiple canopy layers was especially problematic in large riparian polygons with heterogeneous vegetation. We used a 40-percent canopy cover threshold to distinguish between open and closed canopies for both overstory and understory tree layers, as well as the shrub layers. It is possible that the lidar-based classification, trained from the relatively homogeneous quantitative sub-plots, made more accurate classification than was possible in the field.

Large In-Stream Wood and Missing State Classes

To fit the current conditions to the VDDT state class structure (described below), reaches were also assigned to one of three in-stream wood classes: large wood (>20

Table 3—The classification accuracy for current vegetation in the 29 sampled riparian polygons based on a comparison of the lidar-based classification versus the classification made during field sampling

Reach ID	Lidar class[a]	Field class[a]	Type	Size	Canopy	Strata	Shrub	All attributes	Canopy attributes
1169	HMD2D	HMD2D	1	1	1	1	1	1	1
1371	XMD1O	HSO1O				1	1		
6872	XMO1D	HMD2D		1			1		
8808	XSO1D	HSD1O		1		1			
9280	XLO2D	S---O							
10202	XMO1O	XMD2D	1	1					
10444	XMD1O	XMD2D	1	1	1				1
10929	HMD1O	HMD2D	1	1	1				
11448	HMD1O	HMD1O	1	1	1	1	1	1	1
11749	XMD1O	CMD2D		1	1				1
11805	HLD2D	HMD1D	1		1		1		
14925	HMD1O	HMD1D	1	1	1	1			
14957	HLD2D	HMD2D	1		1	1	1		1
15588	HMD1O	HMD2D	1	1	1				1
15764	HMD1O	HMD1D	1	1	1	1			1
15816	HMD2D	HMD2D	1	1	1	1	1	1	1
15898	HMD1D	HMD1O	1	1	1	1			
16594	HMD1O	HMD1D	1	1	1	1			
17049	HMD1D	HMD2D	1	1	1		1		
17061	HLD2D	HMD1D	1		1		1		
17548	HMO1D	HSO2O	1		1				
17807	CLD2D	XMD2D			1	1	1		
18206	HMO2O	HMD2O	1	1		1	1		
18615	XMD1D	S---O							
19058	XSO1D	S---O							
19266	XLD2D	XMD2O	1		1	1			
19726	HMD1O	HMD1D	1	1	1	1			1
19843	HSO1O	S---O					1		
20152	CMO1D	S---D					1		
Number correct			19	17	19	14	13	3	8
Percent correct			66	59	66	48	45	10	28

[a] Classification codes are as follows for each character in the 5 character code:
First character: S=shrub; H=hardwood; C=conifer; X=mixed conifer and hardwood. Second character: S=small; M=medium; L=large.
Third character: O=open; D=dense.
Fourth character: 1=single-story; 2=multi-story.
Fifth character: O=open; D=dense.

in. dbh), small wood (≤20 in. dbh), or no wood. Unfortunately, we were unable to determine the abundance and size of wood present in each stream reach from lidar data. Therefore, reaches within each potential geomorphic type were assigned to each class in the proportion of each wood class determined from field sampling. Additionally, we assumed that local recruitment of in-stream wood would occur in large and giant tree state classes, and therefore, these structural states were assigned to the large wood state classes. Overall, this would tend to overestimate the amount of in-stream wood present in the stream network because little wood was present in many of the sampled reaches even where medium- and large-sized trees were growing in the riparian zone or on lower hillslopes. However, very little of the stream network currently falls into the large or giant state classes. These were seldom observed in the field and none of the sampled plots were field classified into large or giant tree size classes. Thus, errors in the classification

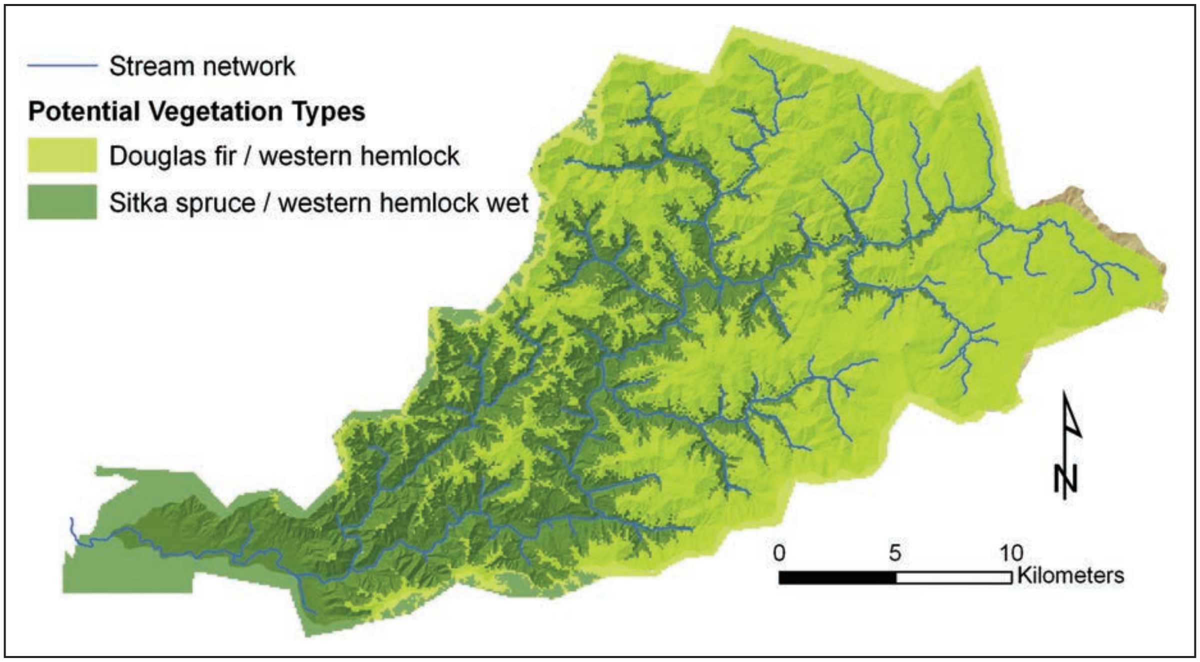

Figure 3—Classification of upland vegetation into Potential Vegetation Types as used in the state and transition models developed for the Wilson River watershed.

of the current conditions caused by assuming that large in-stream wood present in large and giant stands were likely quite small.

The lidar classifications generated a number of structural state classes that were not present in the models we developed. For example, we only simulated open canopy, single-storied stands and closed canopy, multi-storied stands for conifer dominated riparian polygons. Hardwood dominated stands were all simulated as closed canopy, single-storied stands and all mixed conifer and hardwood stands were simulated as closed, multi-storied structural states. Such simplifications are necessary to minimize the complexity of our models and are reasonable approximations of the potential forest structural state classes. The lidar methods we used to classify current conditions, however, were not restricted to just those structural states present in our models. Thus, the lidar classified 144 mixed conifer and hardwood polygons as either open-canopy or as single-storied. These polygons were reclassified into closed canopy multi-storied states. Similarly, the lidar classification generated 194 hardwood-dominated polygons classified either as open canopy or multi-storied all of which were reclassified as closed canopy single-storied states. In total, current conditions in 422 polygons out of the 1554 polygons (27 percent) needed to be reclassified into the most similar state class that occurred in the models.

Aquatic-Riparian State and Transition Models

We intersected the classified stream network map with the potential vegetation map of the Wilson River watershed to identify all possible combinations of channel and vegetation types (table 2). We excluded the coastal plain in the lower watershed from our analyses because the area had been drastically altered by agriculture and development. Models for the remaining area included five geomorphic types in three PVTs: (1) the Sitka spruce/western hemlock wet PVT in the lower parts of the watershed and low elevation riparian zones, (2) the Douglas-fir/western hemlock PVT in the upper parts of the watershed and high elevation riparian zones (fig. 3), and (3) the meadow PVT present only in the extreme eastern portion of the watershed (area of deep-seated landslides in Devils Lake Fork not shown in figure 3 because their spatial extent is too limited to be visible at the scale of the figure). Conceptually, the models do not limit the overstory canopy to a single dominant tree species. For example, in the Sitka spruce/western hemlock wet PVT, we recognize that either mixed species stands, or stands dominated by either Douglas-fir or western hemlock are likely to occur thus we abbreviate this PVT as “sx”, denoting a Sitka spruce—miXed conifer overstory.

We built separate state and transition models for each of the 11 combinations of PVT and geomorphic channel types using the Vegetation Development Dynamics Tool (VDDT; Beukema et al. 2003; http://essa.com/tools/vddt/ accessed 15 November 2011). These VDDT models were developed from upland models for the northern Oregon Coast Range and the Washington Coast Range (please see the ILAP project web page: http://oregonstate.edu/inr/ilap/ as well as the following link for downloads of data, models, and documentation ftp://131.252.97.79/ILAP/Index.html). We expanded these models to include riparian shrub and hardwood state classes, hydrogeomorphic processes, and riparian restoration practices (table 4). We also expanded the pathways and transition probabilities to characterize the historic and current land use activities present in the watershed. The completed models simulated a large number of possible states of a stream reach, from recently disturbed states resulting from stand replacing disturbances such as logging, landslides or wildfire to states where stand replacing disturbances have not occurred for long periods of time.

Individual states within each model are defined on the basis of the potential vegetation type (PVT), the dominant overstory trees, the vegetation structure, and the presence and size of in-stream wood. Tree sizes are based on diameter breast height, in inches, as follows: young 0-1; small 1-10; medium 10-20; large 20-30; giant > 30. In-stream wood is recruited from forested states in two size classes. Small wood constitutes pieces with large-end diameters ≤ 20 inches; large wood is > 20 inches. Thus, in-stream wood recruited from medium-sized tree stands falls into the small-wood class whereas wood from large- or giant-sized tree stands falls into the large-wood state class. Nonforest state classes have tree canopy cover < 15 percent; open canopy state classes have tree canopy cover between 15 percent and 40 percent; closed canopy state classes have tree canopy cover > 40 percent. Open shrub states have shrub cover < 40 percent; closed shrub states have shrub cover > 40 percent. Shrub cover in Sitka spruce/western hemlock wet PVT and Douglas-fir/western hemlock PVT is dominated by *Rubus spectabilis* (salmonberry), while *Salix* spp characterize shrubs in the riparian meadow PVT. In forested states, we assume that conifer-dominated states have open shrub understories whereas alder-dominated or mixed conifer-alder stands have closed shrub understories.

Sitka spruce/western hemlock wet and Douglas-fir/western hemlock PVTs—

Nonforested early seral states used in the models are either barren from post-debris flow conditions or shrub states. Barren conditions are rapidly colonized by salmonberry, transitioning into an open shrub state after 3 years (table 4). Salmonberry grows rapidly and these open shrub states transition to dense shrub states after 2 more years. Wildfires transition directly to the open shrub states which then require 5 years before they reach the dense shrub state class. Forested states can only be initiated from barren or shrub states through tree regeneration. Alder is highly favored early seral tree species in these riparian models (table 4). Conifer regeneration is much lower than that of alder. Further, once salmonberry grows into a dense shrub layer, regeneration rates are reduced by 50 percent for alder and nearly a factor of 10 for conifers. Following conifer regeneration, successional development is simulated as a deterministic process with intermediate seral states defined on the basis of dominant tree sizes rather than age (see table 4). We only simulate open single-story and closed multi-story conifer stands where canopy growth in small, medium, large and giant tree sizes leads to canopy closure (table 4) which is assumed to be accompanied by regeneration of shade-tolerant tree species that form a secondary canopy layer.

Alder regeneration results in a successional sere dominated by alders (table 4). We use a probabilistic transition in year 20 of the small-alder state that forces 25 percent of these state classes into a mixed conifer-alder successional sere. We also simulate relatively slow rates of conifer regeneration in alder-dominated medium-sized tree states.

Table 4—Table of annual transition probabilities and probability multipliers used in the models. (continued)

	Nonforest vegetation			Conifer-dominated forest vegetation				
Vegetative structural state	**Barren**	**Open shrub**	**Dense shrub**	**Young tree**	**Small tree**	**Medium tree**	**Large tree**	**Giant tree**
Age (years)	0-3	0-5	6-200	0-10	11-35	36-65	66-110	111-200+
Base probabilistic transitions								
Tree regeneration (alder)	0.6	0.6	0.3					
Tree regeneration (conifer)	0.04	0.04	0.005					
Canopy growth (open to closed)					0.05	0.03	0.03	0.01
Mixed severity wildfire (open canopy)						0.0027	0.0019	0.0009
Mixed severity wildfire (closed canopy)				0.0045	0.0045	0.0018	0.0027	0.0036
Stand replacing wildfire (open canopy)						0.0023	0.0023	0.0009
Stand replacing wildfire (closed canopy)				0.0045	0.0045	0.0023	0.0023	0.0036
Small wood decay to no wood			20 years					
Large wood decay to small wood			100 years					
Windstorm[1]					$M_{Low,High}$	$M_{Low,High}$	$M_{Low,High}$	$M_{Low,High}$
Transitions controlled with multipliers								
Debris flow source channels		M_3	M_2	M_2	M_2	M_1	M_1	M_1
Debris flow receiving channels	$M_{No,S,L}$	$M_{No,S,L}$	$M_{No,S,L}$	$M_{No,S,L}$	$M_{No,S,L}$	$M_{No,S,L}$	$M_{No,S,L}$	$M_{No,S,L}$
Management controlled with multipliers								
Post-wildfire salvage logging	M	M						
Post-wildfire or logging conifer planting		M						
Pre-commercial thinning				M				
Partial harvest					M	M	M	M
Regeneration harvest					M	M	M	M
Large wood addition				M	M	M		

Table 4—(continued) Table of annual transition probabilities and probability multipliers used in the models.

		Nonforest vegetation		Alder-dominated forest vegetation				
Vegetative structural state	**Barren**	**Open shrub**	**Dense shrub**	**Young tree**	**Small tree**	**Medium tree**	**Large tree**	**Giant tree**
Age (years)				0-5	6-20	21-50		
Probabilistic transitions								
Tree regeneration (conifer)						0.0125		
Alternate succession to mixed conifer – alder stand				0.25 in YR 20				
Stand-replacing wildfire (closed canopy)				0.0045	0.0045	0.0045		
Windstorm					M_{High}	$M_{Low,High}$		
Transitions controlled with multipliers								
Debris flow source channels				M_2	M_2	M_2		
Debris flow receiving channels				$M_{No,S,}$	$M_{No,S,}$	$M_{No,S,L}$		
Management controlled with multipliers								
Hardwood conversion – Plant conifers				M	M			

		Non-forest vegetation		Conifer-alder mixed forest vegetation				
Vegetative structural state	**Barren**	**Open thrub**	**Dense thrub**	**Young tree**	**Small tree**	**Medium tree**	**Large tree**	**Giant tree**
Age (years)						21-65	66-110	110-200
Probabilistic transitions								
Stand-replacing wildfire (closed canopy)						0.0045	0.0045	0.0036
Windstorm						$M_{Low,High}$	$M_{Low,High}$	$M_{Low,High}$
Transitions Controlled with Multipliers								
Debris flow source channels						M_1	M_1	M_1
Debris flow receiving channels						$M_{No, S,L}$	$M_{No, S,L}$	$M_{No, S,L}$

[a] High severity windstorms only occur in the Sitka spruce / western hemlock, wet PVT. See text for details.

Note: the transition probabilities shown here are from the Douglas-fir / western hemlock PVT. The Sitka spruce PVT will use slightly different probabilities. Also, a number of transitions (especially natural disturbance processes where underlying rates are poorly documented and all management-based transitions) rely on a file of multiplier values (shown here as an "M") to determine the rates of these processes in the models. A multiplier of zero effectively turns off the process.

Mixed stands eventually become entirely conifer-dominated after 200 years.

Riparian meadow PVT—
This model characterizes areas of the northeastern portions of the watershed where beaver might be active and contribute to the development of wetlands and ponds. The main difference between this model and the two other PVTs are additional wet meadow/beaver pond states (MeW). The rest of the model (structure and probabilistic transitions) is very similar to the Douglas-fir/western hemlock PVT except that we assume that the non-MeW states are more mesic than structurally similar Douglas-fir/western hemlock states.

The MeW wet meadow/pond state persists when beaver are present and is characterized by grasses/sedges/forbs or riparian shrubs. Floods or beaver extirpation transition wet meadows to relatively drier conditions (MeD). Without reoccurrence of dam building by beaver, MeD states transition to forested stands of Douglas-fir/western hemlock or alder. As in the other PVTs, alder is an early seral tree species with much higher probability of regeneration than conifers. *Salix* spp. dominate in younger alder or conifer states while salmonberry is more abundant in older tree states.

Natural disturbances in all PVTs—
We simulate a variety of probabilistic disturbances (table 4). We simulate several stand replacing disturbances that cause state transitions to the open shrub state. These include stand replacing wildfire and clearcut logging. The overall annual wildfire probability in any forested state is 0.0045 which is equivalent to a 220-year fire return interval. In young- and small-sized tree stands, only stand-replacing wildfire occurs. In stands with larger trees, both mixed-severity and stand-replacing fires occur, and the actual probabilities vary with tree size and canopy closure. Mixed-severity fires transition closed-canopy state classes to open canopy states or maintain pre-existing open-canopy states. Mixed-severity fires also drive recruitment of wood into the streams—recruiting small wood from the medium-sized states and large wood from the large- and giant-sized states.

High severity wind storms are also simulated as stand replacing disturbances but only occur in the low-elevation, Sitka spruce/western hemlock wet PVT—thus preferentially affecting wet sites in low-elevation mountain valleys located nearest to the Pacific coast. We parameterized the models with high-severity windstorm probabilities equal to 0.0083 per year (for a return interval of 120 years). We assume the shrub layer will be minimally disturbed by high-severity windstorms so that the postdisturbance stand inherits an open or dense state class from the predisturbance state class.

State transitions resulting from low-severity wind storms are similar to those caused by mixed-severity fire in that these wind storms transition closed-canopy state classes to open canopy states or maintain preexisting open-canopy states. They also drive recruitment of small wood from the medium-sized states and large wood from the large- and giant-sized states. We parameterized the models with high-severity windstorm probabilities equal to 0.0100 per year (for a return interval of 100 years).

We only simulate decay and loss of large, in-stream wood in the dense shrub state class where we require 100 years for the large-wood state class to transition into a small-wood state, and 20 years for a small-wood state class to transition into a no-wood state class. Wood decay cannot be easily tracked in the other state classes because there are multiple transition pathways and disturbances that can recruit additional wood and the VDDT modeling software prevents tracking the age of specific attributes independently of the age of the underlying state class.

The occurrence of debris flows are controlled using a multiplier file. We start by assuming that the probability of landslide-caused debris flows is limited by the potential rate of hillslope hollow refilling which suggests that landslides might occur approximately 1 in 500 years from colluvial hillslope hollows. This would give an expected base rate of debris flows of 0.002 per year. There is substantial evidence, however, that debris flows are more likely to occur soon after stand-replacing disturbances. Thus, for channel types where debris flows are likely to originate (cascade and cascade with wood-forced step pools), we created three categories: Debris Flow1 (multiplier M_1 in table 4) occurs in mature and old-growth forest and accounts for 10 percent of all debris flows; Debris Flow2 (multiplier M_2 in table 4) occurs in dense shrub, young, and small forest state classes and accounts for 30 percent of all debris flows; Debris Flow3 (multiplier M_3 in table 4) occurs only in the open shrub state class which results from wildfire or clearcutting and accounts for 60 percent of all debris flows. Because the underlying base probability given to all debris flows in the state-and-transition models is 0.01, we use the following multipliers to drive debris flow transitions in models for cascade or cascade-with-wood-forced-step channels: M_1=0.02; M_2=0.06; M_3=0.12.

Larger channels lower in the network (step-pool, planebed, and pool-riffle) have longitudinal gradients too shallow for origination of landslides. Instead, they are impacted by debris flows moving down the stream network. Because many headwater channels converge to form larger streams, and because the larger stream can be impacted by debris flows in any of the headwater channels, the probability of a debris flow increases. Consequently, we assumed that debris flows impacted step-pool channels 1 in 100 years and 1 in 50 years for planebed and pool-riffle channels.These debris flows may originate in an area lacking large wood and deposit only sediment, or may travel through the reach removing all large wood. Alternatively, they could deposit either small wood or large wood. Thus we created three categories: Debrisflow no wood (multiplier M_{No} in table 4) where the debris-flow-impacted channel is left free of wood; Debrisflow small wood (multiplier M_S in table 4) where the debris flow impacted channel is left with abundant small wood; Debrisflow large wood (multiplier M_L in table 4) where the debris-flow-impacted channel is left with abundant large wood. In the simulations reported here, these three classes of debris flows were given equal weightings. Again, because the underlying base probability given to all debris flows in the state-and-transition models is 0.01, we use the following multipliers to drive debris flow transitions in models for all step-pool channels: $M_{NO} = M_S = M_L =$ 0.3300. We use the following multipliers for all planebed and pool-riffle channels: $M_{NO} = M_S = M_L = 0.6700$. Future model runs can be made iteratively, and the relative proportion of no wood, small wood, and large wood debris flows could be based on the tree size and large wood abundance in the debris flow source areas.

Management transitions in all PVTs—
The models we developed include a large number of possible management practices. Logging transitions (post-wildfire salvage logging, precommercial thinning, partial harvest and regeneration harvest, or clearcutting) were inherited from the upland models we used as a starting point for the aquatic-riparian models (table 4). In all cases, these transitions are initialized with a base probability of 0.0100 and must be controlled using an external multiplier file. We have not simulated forest harvest in any riparian stands so in the simulations reported here, all forest harvest transitions probabilities were set to zero.

The models also include several planting or restoration transitions, including planting of conifers in the open shrub state class following stand-replacing disturbances, large wood additions to the stream, and hardwood conversion of small alder stands by planting of conifers. These restoration transitions are also initialized with a base probability of 0.0100 and must be controlled using an external multiplier file. Additional management practices or prescriptions could be added to the models if need is demonstrated by managers or model users. Similarly, natural disturbance pathways could be edited and transition probabilities altered with new probabilities, or modified by using static or temporal multipliers.

Channel Conditions and Aquatic Habitat Quality

We used a 4-factor scale for each state class in the models to qualitatively rank their channel morphologic conditions: shade, erosion, undercut banks, large wood, pools, large pools, off-channel habitat, width-depth ratio, and riparian shrub abundance. We inferred the relative abundance of large wood, pools, undercut banks, and erosion from the cover type and structural stage of each state class in the models. These variables were then used in an expert systems model to rank the habitat quality (poor, fair, good, excellent) for migration, spawning, summer and winter rearing of coho salmon and steelhead. We assumed that coho habitat would be characterized by low gradient reaches (< 3 percent gradient), abundant large pools, and low erosion (low concentration of fine sediment) for spawning.

We used the abundance of large pools as an indicator of pool-riffle morphologies that would provide appropriate spawning riffles. Where pools were lacking, low -gradient reaches were assumed to be in a plane-bed state, with few distinct riffles. We assumed that Coho rearing habitat would be characterized by abundant pools, a combination of either undercut banks or large wood, and abundant off-channel habitat in areas with low erosion (low concentration of fine sediment). Thus, states with low gradient (i.e. pool-riffles) and abundant in-stream large wood, either recruited by stand-altering disturbances or self-recruited from large and giant trees, were assumed to provide the most favorable coho habitat.

We assumed that steelhead habitat would encompass nearly all coho habitat in low gradient reaches (i.e. pool-riffle morphologies) but would also extended into higher gradient reaches (including step-pool reaches) as long as pools and in-stream wood were abundant. We assumed that steelhead spawning requirements would be similar to those of coho, that is, they would utilize riffles in pool-riffle reaches where large pools were abundant and erosion (concentration of fine sediment) was low. We assumed that steelhead rearing habitat would be much more extensive within the watershed because this species was better able to occupy steeper reaches (i.e., > 3 percent gradient) with fast flowing water and little off-channel habitat. Also, steelhead typically spend two years rearing in freshwater instead of the single year that is the norm for coho. Thus we assumed that steelhead would be larger bodied in their second year, and would require larger pools and deeper water than in their first year.

We combined our qualitative habitat rankings with an independent evaluation of potential habitat quality, using Intrinsic Potential (IP) models (Burnett et al. 2007). IP scores are based on channel gradient, valley floor width, and drainage area and thus reflect the underlying physical "potential" to support the species of interest. The IP scores do not change over time, regardless the type and magnitude of disturbances that may alter other channel characteristics that influence the current quality of the stream habitat. We used the IP scores as a coarse filter through which we could identify portions of the stream network that had the potential to provide quality habitat for rearing, i.e., reaches where coho IP ≥ 0.60 (~18 km of the stream network) and steelhead IP ≥ 0.75 (~150 km of the stream network). Thus, large portions of the watershed, especially the coastal plain which has been converted to agricultural uses, mainstem reaches confined by bedrock gorges or high alluvial terraces, and headwater reaches too steep to support fish were excluded from our analyses.

Analysis and graphical display of model output— We developed the 4-factor ranking scale for both channel attributes and fish habitat quality in MS Excel but using spreadsheet templates from VDDT and then imported the ranked attributes into the VDDT models. Thus, the native graphic capabilities of VDDT or PATH (Path Landscape Model, VDDT's sister state-and-transition simulation model; http://www.apexrms.com, accessed 15 November, 2011) and other analytical tools can be used to analyze the model outputs. However, we found it easier to conduct these analyses outside of the VDDT/PATH platform where we could code SAS (Statistical Analysis Software) to perform specific detailed analyses needed to answer the questions in which we were interested. Further, we coded SAS to format output datasets that could be pasted directly into a graphic template in SigmaPLOT and thus quickly analyze and display results of individual model runs.

Model Application

The state and transition models were applied to the mountainous portion of the Wilson River watershed (500 km^2) in the northern Oregon Coast Range to examine: (1) current conditions relative to the historic condition; (2) likely trajectories of aquatic and riparian habitats given current and expected land-use practices; (3) the potential of passive restoration to meet recovery goals; and (4) the potential of active restoration to accelerate recovery. As a first step in our analysis, we simulated the Tillamook Burns to evaluate the ability of the models to successfully "hindcast" current conditions resulting from forest regrowth following these large, stand-replacing fires. We then used the models to compare future projections of habitat quality resulting from

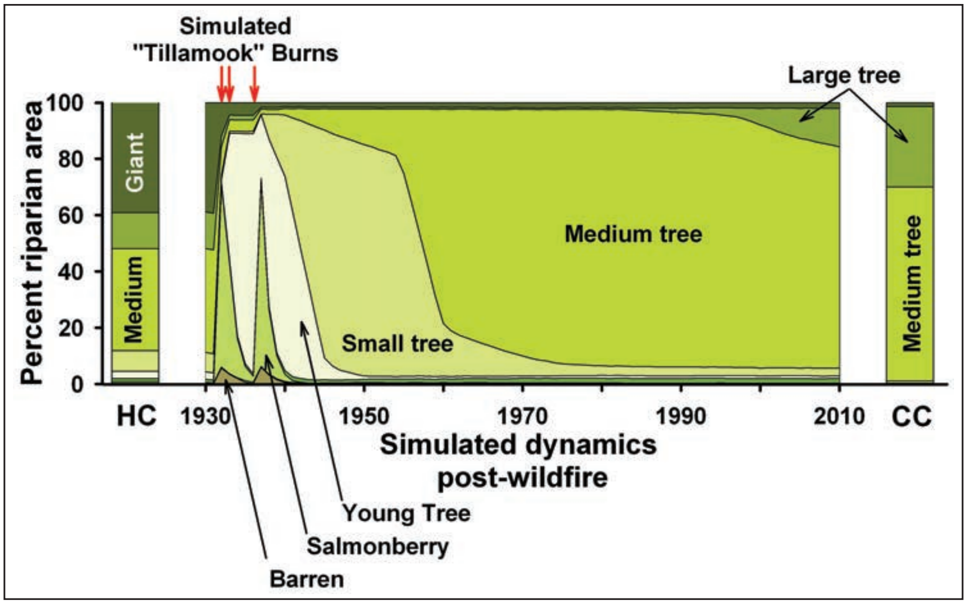

Figure 4—Comparison of historic condition (HC), the time series of changes resulting from the Tillamook Burns and subsequent forest regrowth through 2010, and the lidar-derived current condition (CC) for approximately 2010. The model projection includes a 10-year period from 1930 to 1940 where the watershed burned three times (red arrows), with each burn covering approximately 75 percent of the watershed. During the post-fire recovery (1940–2010), stand-replacing wildfires did not occur, but the models continued to simulate background rates of wind disturbance, mixed-severity wildfire, and debris flows.

active restoration with large wood addition to that resulting from passive restoration.

Simulating the Effect of the Tillamook Burns

The history of the Tillamook Burns—a series of large stand replacing wildfires that burned large portions of the northern Oregon Coast Range in 1933, 1939, 1946, and 1951—provides an opportunity to examine the ability of our state and transition models to simulate a time series of episodic disturbance and subsequent recovery of the riparian forests. We lack detailed records of the conditions of the Wilson River watershed prior to these major fires. However, large portions of the watershed were burned in high-intensity fires that essentially reset vegetation structure and composition to post-wildfire states. Thus, we initialized our model runs with initial conditions reflecting the long-term average historical condition of riparian vegetation within the watershed. The historic condition was projected from a 1000-year model run in which all anthropogenic effects were turned off and natural disturbance rates reflected the presumed historical rates of wildfires, windstorms, and debris flows. We lack detailed records of the exact portions of the Wilson River watershed burned in the Tillamook fires as well as historical records of postfire salvage logging and efforts to replant the burned areas. We do know that the 1933 fire was the largest of the "Tillamook Burns," so we used a series of temporal multipliers to force major wildfires in 1933 and 1934 and again in 1938. Each of these fires burned approximately 75 percent of the watershed so that by the late 1930s the structure and composition of the watershed had been nearly entirely reset to the earliest seral stages.

We simulated postfire recovery (1940–2010) by preventing stand-replacing wildfires (which did not occur over this time period), but continued to simulate background disturbances from wind, mixed-severity wildfire, and debris flows. Because salmonberry is a highly successful early-seral shrub throughout the northern Oregon Coast Range and resprouts readily after wildfire, in our models, wildfires forced transitions to salmonberry-dominated state classes (fig. 4). Subsequently alder rapidly colonized these states

Table 5—Summary table showing the percent of the riparian area in each vegetation composition and structural group within the Wilson River watershed

							Non-	Salmon-	Alder	Alder	Alder	Mixed	Mixed
Mixed							Conifer	Conifer	Conifer	Conifer	Conifer		
Time step	Forest	berry	young	small	medium	medium	large	giant	young	small	medium	large	giant
HC	1.1	0.8	2.4	6.80	18.96	16.5	11.12	12.86	0.2	0.5	0.8	1.76	26.18
Post-burn	6.9	66.2	21.6	0.3	0.8	0.8	0.6	0.6	0.9	0	0.1	0.2	1.1
1940	1.6	3.2	65.2	21.6	1.2	1	0.5	0.4	3.8	0.2	0.1	0.2	1.1
1950	1.3	0.4	0.9	78.5	8.7	3.9	0.5	0.5	0.3	3.8	0	0.2	1.1
1960	1.5	0.4	0.9	14.7	60.4	15.7	0.5	0.5	0.1	4	0.1	0.1	1.2
1970	1.6	0.5	0.8	4.5	61.7	24.2	0.5	0.5	0	2.5	1.7	0.1	1.2
1980	1.6	0.5	0.9	2.7	56.3	31.1	0.5	0.5	0	0.8	3.6	0.1	1.2
1990	1.7	0.4	0.9	2.7	50.4	36	1.4	0.6	0.1	0.5	4.1	0.1	1.3
2000	1.7	0.4	0.9	2.6	45	38	4.6	0.6	0	0.3	3.4	1.3	1.3
2010	1.6	0.4	0.9	2.6	40.3	36.1	11.1	0.6	0.1	0.2	2.2	2.7	1.3
LIDAR-CC	0.3	0	0	0.1	42.2	11.4	29.4	0.5	0	0.5	5	10.1	0.6

Note: The data shown here subdivide the coarser vegetation classes shown in figure 4. HC denotes the simulated long-term average condition of the stream network resulting from a long-term (1,000-year) simulation of natural disturbance and plant succession. Post-burn denotes the composition and structure of the riparian zone in the year following the last simulated burn. LIDAR-CC denotes the current condition of the riparian zone, based on the lidar-derived vegetation structural classes and subsequent classification into model state classes.

resulting in a rapid shift toward alder dominance, followed by growth and aging of established trees over time (table 5). By the end of the simulation period in 2010, forest structure and composition resembled the 2010 lidar-derived current conditions (fig. 4).

Current vegetation (both simulated and lidar-derived), however, is markedly distinct from the long-term average historic condition (fig. 4, table 5). Current conditions (CC; fig. 4) were determined through classification of lidar imagery. Giant conifer (DBH > 30 inches) dominated stands are notably lacking in the riparian zone. Historically, our simulations project that some 25 percent of the stream network would have supported riparian vegetation dominated by conifers larger than 30 inches DBH. Conversely, alder-dominated stands and mixed conifer-alder stands of medium- or large-sized trees are overrepresented in the riparian zone (fig. 4). These trends are expected, given the history of large, stand-replacing wildfires within the watershed.

A more detailed analysis of forest composition, separating the forest types into alder-dominated forest, conifer-dominated forests, and mixed forests where conifers are beginning to over-grow previously alder-dominated forests, is shown in table 5. There are some discrepancies between the simulated structure and composition in 2010, compared to the lidar-derived current vegetation. For example, we under predict the amount of large, conifer-dominated forest (table 5). However, much of the area within the Tillamook Burn was planted with conifers in the decade following the burns. We did not simulate postdisturbance planting in our model runs. First, our models only allow postdisturbance planting over a short time window following disturbance which is typical of Burned Area Emergency Response (BAER) treatments currently employed within the region. Second, we do not know if the riparian zones were successfully planted in the Tillamook Burn area. Certainly, our observations in the field and the composition of the lidar-derived current vegetation are generally in agreement with the simulation results which indicate that large areas of the riparian zone remain in alder-dominated stands. Overall, we conclude that the models, as parameterized, provide an

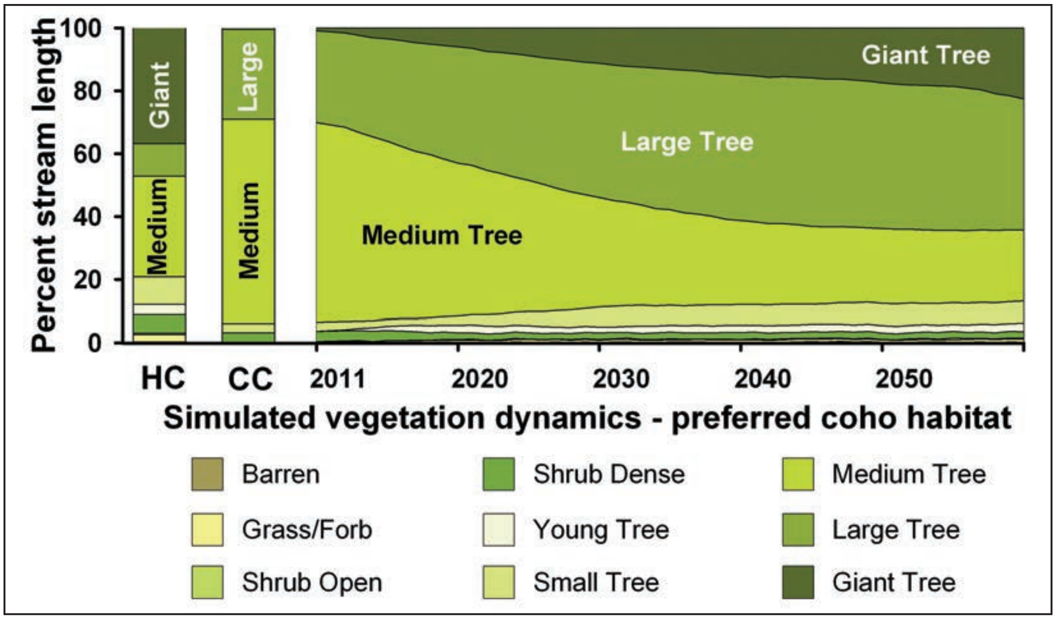

Figure 5a—Comparison of historical condition, current condition, and projected future conditions of the riparian vegetation resulting from passive restoration (i.e., all anthropogenic activities turned off) in areas where the intrinsic potential score for coho is greater than 0.60.

acceptable simulation of the riparian vegetation dynamics in the riparian zones of the Wilson River watershed.

Changes in Coho and Steelhead Habitat

Coho—

Only 18 km of the stream network within the mountainous portions of the Wilson River watershed have high intrinsic potential to provide quality rearing habitat for juvenile coho salmon (IP score ≥ 0.60). Comparisons of the simulated historical condition and with lidar-derived current condition of riparian vegetation show large departures from historical conditions. The historical condition (HC) was projected from 500-year model runs in which all anthropogenic effects were turned off but natural disturbances continued to occur. Current conditions (CC) were determined through classification of lidar imagery. Under current conditions, giant-tree structural states are almost entirely lacking and nearly two-thirds of the riparian areas are dominated by medium-sized tree structural states (fig. 5a). Simulations of the historical condition suggest that nonforest vegetation comprised as much as 10 percent of the riparian zone. Today, nonforest vegetation comprises less than 5 percent of the riparian zone. Changes within the watershed have also substantially influenced the quality and abundance of rearing habitat available for coho salmon (fig. 5b). Our historical simulation suggests that nearly two-thirds of the potentially useable habitat would have been ranked as good or excellent quality. Today, less than 25 percent of that stream habitat is ranked as good or excellent.

Future conditions were projected from the aquatic-riparian VDDT models with all anthropogenic activities turned off (i.e., no forest harvest in riparian zones, no salvage logging, and no riparian planting or other restoration treatments). This simulation is effectively a "passive restoration" scenario where no active management occurs. Simulations suggest that, over time spans of 5 to 10 years, changes in vegetation structure are relatively slow. Over the longer term, in the absence of episodic disturbances, the growth of conifers in mixed stands will lead to a slow but steady increase in the abundance of large trees. However, even after another 50 years (by ca. 2060) riparian forest conditions will still remain distinct from their historical conditions (fig. 5a). Similar patterns are seen in the projections for habitat abundance and quality for coho salmon, with changes accumulating slowly, but steadily, so that conditions are markedly improved after 50 years. However,

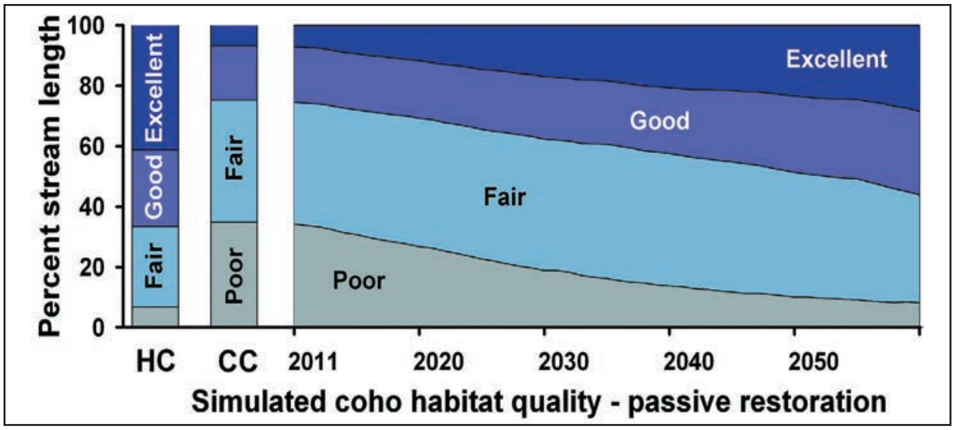

Figure 5b—Comparison of rearing habitat quality under historicall, current, and projected future conditions resulting from passive restoration in areas where the intrinsic potential score for coho is greater than 0.60.

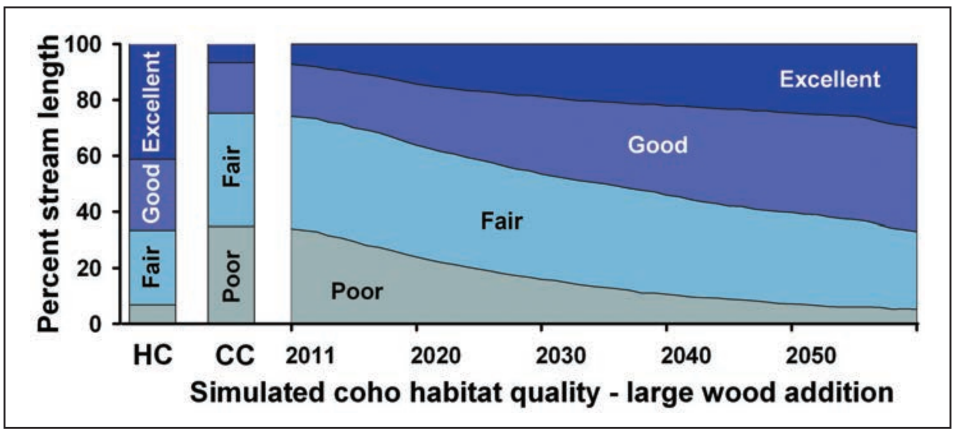

Figure 5c—Comparison of rearing habitat quality under historic, current, and projected future conditions resulting from an active restoration from large wood addition in areas where the intrinsic potential score for coho is greater than 0.60. Note that large wood addition has no effect on the structure and composition of the adjacent riparian vegetation, thus vegetation structure is not shown for this simulation.

even after 50 years of "passive restoration," comparison with the historical condition shows that there is substantially less habitat ranked as excellent and more ranked as fair (fig. 5b) than in the simulated historical condition.

Steelhead—

The portions of the stream network with the highest potential to provide high-quality rearing habitat for steelhead (IP score > 0.75) are much more extensive than for coho, encompassing most of the modeled reaches of the mainstem Wilson River as well as all of the larger tributaries within the watershed. Collectively, more than two-thirds of the modeled stream network has the potential to provide high-quality rearing habitat for steelhead.

Comparisons between the simulated historic condition and lidar-derived current condition of riparian vegetation for steelhead are very similar to those for coho salmon in which giant-tree structural states are almost entirely lacking and nearly two-thirds of the riparian areas is dominated by medium-sized tree structural states (fig. 6a). The quality and abundance of rearing habitat available for steelhead under current conditions is also substantially different from the simulated historical condition (fig. 6b). Our historical simulation suggests that nearly two-thirds of the high IP

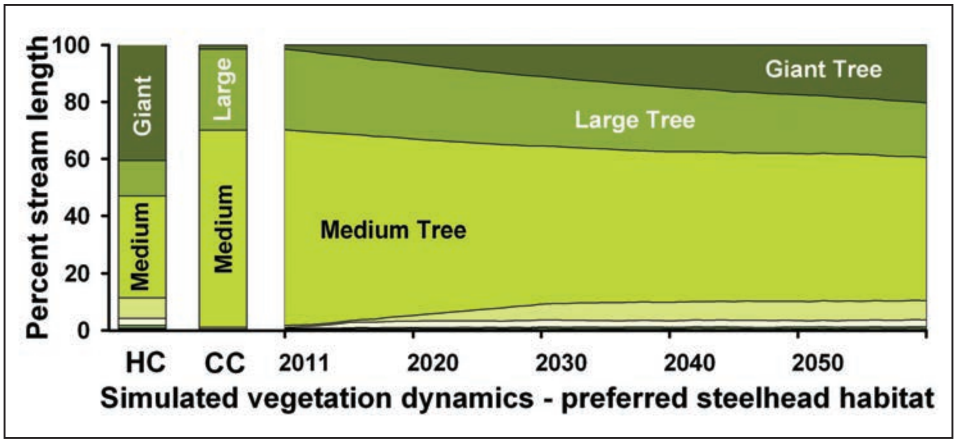

Figure 6a—Comparison of historic condition, current condition, and projected future conditions of the riparian vegetation resulting from passive restoration (i.e., all anthropogenic activities turned off) in areas where the intrinsic potential score for steelhead is greater than 0.75. Legend follows figure 5a.

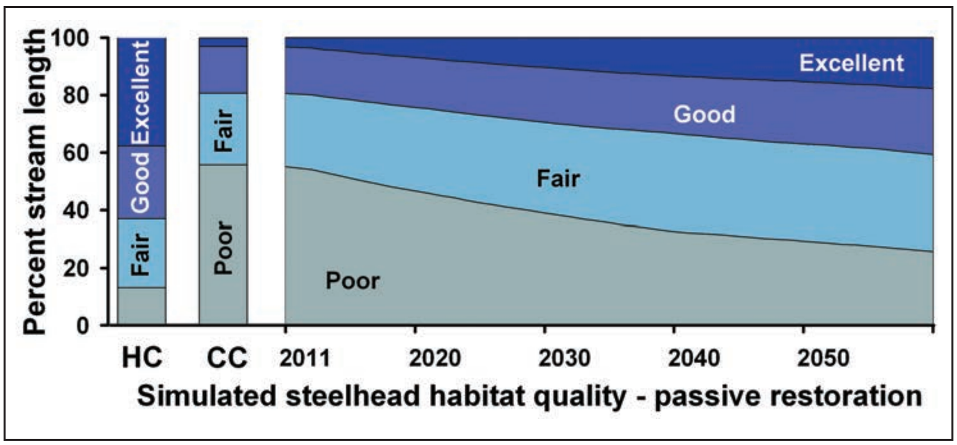

Figure 6b—Comparison of rearing habitat quality under historic, current, and projected future conditions resulting from passive restoration in areas where the intrinsic potential score for steelhead is greater than 0.75.

habitat would have been ranked as good or excellent habitat quality. Today, only 20 percent of that stream habitat is ranked as good or excellent.

Simulations of passive restoration suggest that, over the short term, changes in vegetation structure are relatively slow. Over the longer term, the models simulate substantial growth of riparian trees, however, even after another 50 years (by ca. 2060) riparian forests remain distinct from their historical conditions (fig. 6a). As with coho, similar patterns are seen in the projections for habitat abundance and quality for steelhead, with changes accumulating slowly, but steadily, so that conditions are markedly improved after 50 years. However, even after 50 years of "passive restoration," comparison with the historical condition shows that there is substantially less habitat ranked as excellent and more ranked as fair or poor (fig. 6b) than in the simulated historical condition.

Stream Restoration Through Large Wood Augmentation

Our model simulations project substantial recovery is likely to occur over the next 50 years in the absence of major episodic disturbance, however, even after 50 years, the quality and abundance of stream habitat for coho and

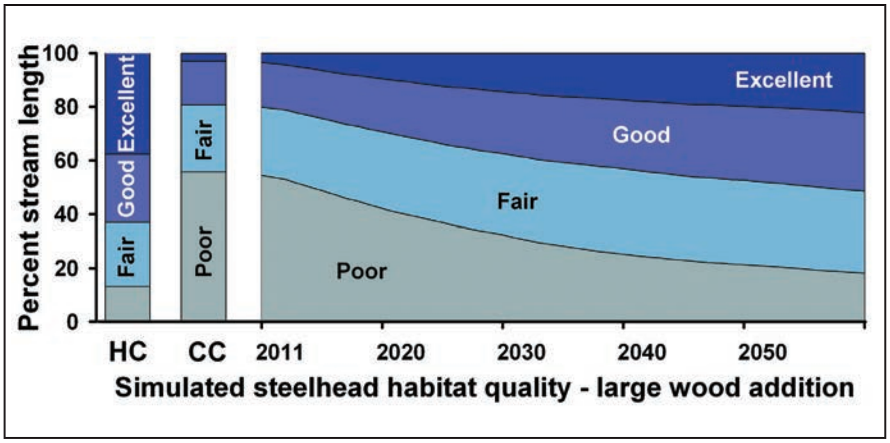

Figure 6c—Comparison of rearing habitat quality under historic, current, and projected future conditions resulting from active restoration scenario with large wood addition in areas where the intrinsic potential score for steelhead is greater than 0.75. Note that large wood addition has no effect on the structure and composition of the adjacent riparian vegetation, thus vegetation structure is not shown for this simulation.

steelhead remains distinct from the simulated historical condition. One active restoration approach would be to add large wood to stream reaches where it is currently lacking to accelerate the recovery of habitat quality. The initial conditions we used to start our model runs for the 18 km of river with high intrinsic potential for coho salmon indicated that 61 percent of those 18 km had little or no stream wood and 24 percent had abundant large wood at the beginning of our simulation (ca. 2010). In the active recovery scenario, we simulated active large wood addition, treating approximately 1 km of stream network per decade. After 50 years, the portion of those 18 km where large wood was abundant increased from 53 percent to 64 percent. These large wood addition treatments, however, led to a small increase in the availability of coho rearing habitat ranked good or excellent after 50 years. Some 57 percent of the stream network was ranked good or excellent under the passive restoration scenario and 67 percent ranked in those categories in the active restoration scenario (fig. 5b versus 5c). Because the availability of high-quality habitat for coho is presently very limited within the Wilson River watershed, treating only 5 km of stream channel through large wood addition results in a modest improvement in simulated habitat quality.

We conducted a similar series of model simulations for the 150 km of stream network with high intrinsic potential to support steelhead. Our simulations showed that to get an improvement similar to coho in the amount of habitat ranked good or excellent required treatment of approximately 44 km of stream channel which increased the amount of the stream network ranked good or excellent from 41 percent under passive restoration to 52 percent under active restoration over the 50-year model simulation (fig. 6b versus 6c). The active restoration scenario for steelhead would be much more expensive than for coho because it would require adding large wood to approximately 9 km of stream per decade.

The abundance of large wood was not readily quantified from the remote sensing techniques employed in this study. We did make estimates of large wood abundance from our field sampling plots (n = 29) which allowed us to specify the initial conditions for our model simulation. However, we emphasize that our 29 sample plots are too few to realistically estimate the abundance of large wood. Actual stream inventory data would help set more realistic initial conditions for our model simulation.

Discussion

The results presented here demonstrate the utility of our state and transition models for exploring a variety of questions related to landuse decisions and the effect of alternative management scenarios on riparian vegetation, channel morphology, and stream habitat condition for salmonids.

The restoration scenarios examined here represent only a few of the large number of management questions that could be explored using these models.

State and transition models are relatively "transparent" in that other users can pick up a package of existing models, and with a minimum effort begin working with those models. This ease of use is facilitated by the fact that the VDDT and PATH software (http://www.apexrms.com/path, accessed 15 November 2011) needed to run these models are publicly available and relatively easy to use. And while the size of some of our aquatic-riparian state and transition models may make them appear daunting at first, the software user interface makes it relatively easy to revise the models to meet a wide variety of alternative assumptions. The true value of these models is that alternative assumptions or "alternative management scenarios" can then be readily tested and the model outputs used to provide hypotheses of likely outcomes to explore the ways in which policy decisions may influence the future condition of riparian zones.

Our models are broadly portable. We developed models specifically for the Wilson River watershed in the northern Oregon Coast Range. However, similar potential vegetation and geomorphic types occur throughout the central and northern Oregon as well as the southern Washington Coast Range. Consequently, our models are likely to be directly applicable to these larger regions. Further, the general model structures and the rather exhaustive list of transition processes included in the models provides a template from which models for other areas within the region could be readily constructed.

Although the results of our model simulations have appeared reasonable wherever data were available for comparison, we caution that these comparisons do not provide detailed validation of all the factors simulated in our models. Consequently, the results of the model simulations should be interpreted cautiously. The models are not intended to provide detailed predictions of specific outcomes at the scale of a single reach or for a specific restoration project involving 100s or a few kilometers of stream channel. Rather, the results of the model simulations should be interpreted as hypotheses of likely outcomes from management directions at the scale of a large watershed (one or several 5th-field hydrologic units or HUC5s) or a large portion of a USFS Ranger District.

References

Beukema, S.J.; Kurz, W.A.; Pinkham, C.B.; Milosheva, K.; Frid, L. 2003. Vegetation Dynamics Development Tool, User's Guide, Version 4.4c. Vancouver, BC, Canada: ESSA Technologies Ltd. 239 p.

Breiman, L. 2001. Random Forests. Machine Learning, 45:5–32. Burnett, K.M.; Reeves, G.H.; Miller, D.J.; Clarke, S.; Vance-Borland, K.; Christiansen, K. 2007. Distribution of salmon-habitat potential relative to landscape characteristics and implications for conservation. Ecological Applications. 17: 66–80.

Castro, J.M.; Jackson, P.L. 2001. Bankfull discharge recurrence intervals and regional hydraulic geometry relationships: patterns in the Pacific Northwest, USA. Journal of the American Water Resources Association. 37: 1249–1262.

Federal Caucus. 2000. Vols. 1–2. Conservation of Columbia basin fish, final basinwide salmon recovery strategy. Portland, OR: Federal Caucus/Bonneville Power Administration. http://www.salmonrecovery.gov/Final_Strategy_Vol_1.pdf, http://www.salmonrecovery.gov/Final_Strategy_Vol_2.pdf. (June 9, 2003).

Gatziolis, D.; Fried, J.S.; Monleon, V.S. 2010. Challenges to estimating tree height via LiDAR in closed-canopy forests: A parable from western Oregon. Forest Science. 56: 139–155.

Hudak, A.T.; Crookston, N.L.; Evans, J.S.; Hall, D.E.; Falkowski, M.J. 2008. Nearest neighbor imputation of species-level, plot-scale forest structure attributes from LiDAR data. Remote Sensing of Environment. 112: 2232–2245.

Montgomery, D.R.; Buffington, J.M. 1997. Channel-reach morphology in mountain drainage basins. Geological Society of America Bulletin. 109: 596–611.

Montgomery, D.R.; Buffington, J.M. 1998. Chapter 2: Channel processes, classification, and response. In: R.J. Naiman and R.E. Bilby, eds. River Ecology and Management—Lessons from the Pacific Coastal Ecoregion. New York: Springer-Verlag: 13–42.

National Research Council (NRC). 2002. Riparian areas: functions and strategies for management. Washington, DC.: National Academy Press. 428 p.

Nehlsen, W.; Williams, J.E.; Lichatowich, J.A. 1991. Pacific salmon at the crossroads: Stocks at risk from California, Oregon, Idaho and Washington. Fisheries. 16: 4–21.

Pflugmacher, D.; Cohen, W.B.; Ohmann, J.L.; Kennedy, R.E. 2011. Final report to the Oregon Watershed Enhancement Board, for grant OWEB # 208-8007-5781. Mapping Current Conditions and Modeling the Dynamic Responses of Riparian Vegetation and Salmon Habitat in Oregon: Mapping Component. Submitted 6 June 2011.

U.S. Department of Agriculture, Forest Service; U.S. Department of the Interior, Bureau of Land Management. 2000. Interior Columbia basin supplemental draft environmental impact statement. The Interior Columbia Basin Ecosystem Management Project. Washington, DC: U.S. Government Printing Office. [Irregular pagination].

U.S. Geological Survey and U.S. Department of Agriculture, Natural Resources Conservation Service. 2009. Federal guidelines, requirements, and procedures for national Watershed Boundary Dataset: U.S. Geological Survey Techniques and Methods 11-A3, 55 p.